

## Comparison of static chambers to measure CH<sub>4</sub> emissions from soils

Mari K. Pihlatie<sup>a,\*</sup>, Jesper Riis Christiansen<sup>b,t,1</sup>, Hermann Aaltonen<sup>a,c</sup>, Janne F.J. Korhonen<sup>a</sup>, Annika Nordbo<sup>a</sup>, Terhi Rasilo<sup>d</sup>, Giuseppe Benanti<sup>e</sup>, Michael Giebels<sup>f</sup>, Mohamed Helmy<sup>e</sup>, Jatta Sheehy<sup>g,h</sup>, Stephanie Jones<sup>i,j</sup>, Radoslaw Juszczak<sup>k</sup>, Roland Klefoth<sup>l</sup>, Raquel Lobo-do-Vale<sup>m</sup>, Ana Paula Rosa<sup>n</sup>, Peter Schreiber<sup>o,p</sup>, Dominique Serça<sup>q</sup>, Sara Vicca<sup>r</sup>, Benjamin Wolf<sup>s</sup>, Jukka Pumpanen<sup>d</sup>

<sup>a</sup> Department of Physics, Division of Atmospheric Sciences, FI-00014 University of Helsinki, Finland

<sup>b</sup> Division of Biomass & Ecosystem Science, University of Copenhagen, Denmark

<sup>c</sup> Finnish Meteorological Institute, P.O. Box 503, 00101 Helsinki, Finland

<sup>d</sup> Department of Forest Sciences, FI-00014 University of Helsinki, Finland

<sup>e</sup> School of Biology and Environmental Science, University College Dublin, Dublin 4, Ireland

<sup>f</sup> Leibniz-Centre for Agricultural Landscape Research, Institute of Landscape Biogeochemistry, Eberswalder Str. 84 D-15374 Müncheberg, Germany

<sup>g</sup> MTT Agrifood Research Finland, Plant Production Research, FI-31600 Jokioinen, Finland

<sup>h</sup> Department of Plant Sciences, University of California, Davis, CA 95616, USA

<sup>i</sup> Scottish Agricultural College, King's Buildings, West Mains Road, Edinburgh EH9 3JG, UK

<sup>j</sup> Centre for Ecology and Hydrology (CEH), Edinburgh, Bush Estate, Penicuik, Midlothian EH26 QB, UK

<sup>k</sup> Meteorology Department, Poznan University of Life Sciences, Piatkowska 94, 60-649 Poznan, Poland

<sup>l</sup> Wageningen UR, Environmental Sciences, Soil Science Centre, P.O. Box 47, 6700 AA Wageningen, The Netherlands

<sup>m</sup> Agronomy Institute, Technical University of Lisbon, Tapada da Ajuda 1349-017, Lisboa, Portugal

<sup>n</sup> Centre for Environmental Biology, Faculty of Sciences, University of Lisbon, Lisboa, Portugal

<sup>o</sup> University of Hamburg, KlimaCampus, Institute of Soil Science, Allende-Platz 2, 20146 Hamburg, Germany

<sup>p</sup> Institute of Botany and Landscape Ecology, Ernst Moritz Arndt University Greifswald, Grimmer Str. 88, 17487 Greifswald, Germany

<sup>q</sup> Laboratoire d'Aérodynamique – Observatoire Midi-Pyrénées, FR-31400 Toulouse, France

<sup>r</sup> University of Antwerp, Research Group of Plant and Vegetation Ecology, Universiteitsplein 1, 2610 Wilrijk, Belgium

<sup>s</sup> Institute for Meteorology and Climate Research (IMK-IFU), Karlsruhe Institute of Technology, Kreuzeckbahnstraße 19, 82467 Garmisch-Partenkirchen, Germany

<sup>t</sup> Department of Forest Sciences, Faculty of Forestry, University of British Columbia, Main Mall 2424, V6T1Z4, Vancouver, BC, Canada

### ARTICLE INFO

#### Article history:

Received 29 September 2011

Received in revised form 30 October 2012

Accepted 12 November 2012

#### Keywords:

Methane

Soil

Fluxes

Static chamber

Flux calculation

### ABSTRACT

The static chamber method (non-flow-through-non-steady-state chambers) is the most common method to measure fluxes of methane (CH<sub>4</sub>) from soils. Laboratory comparisons to quantify errors resulting from chamber design, operation and flux calculation methods are rare. We tested fifteen chambers against four flux levels (FL) ranging from 200 to 2300 μg CH<sub>4</sub> m<sup>-2</sup> h<sup>-1</sup>. The measurements were conducted on a calibration tank using three quartz sand types with soil porosities of 53% (dry fine sand, S1), 47% (dry coarse sand, S2), and 33% (wetted fine sand, S3). The chambers tested ranged from 0.06 to 1.8 m in height, and 0.02 to 0.195 m<sup>3</sup> in volume, 7 of them were equipped with a fan, and 1 with a vent-tube. We applied linear and exponential flux calculation methods to the chamber data and compared these chamber fluxes to the reference fluxes from the calibration tank.

The chambers underestimated the reference fluxes by on average 33% by the linear flux calculation method ( $R_{lin}$ ), whereas the chamber fluxes calculated by the exponential flux calculation method ( $R_{exp}$ ) did not significantly differ from the reference fluxes ( $p < 0.05$ ). The flux under- or overestimations were chamber specific and independent of flux level. Increasing chamber height, area and volume significantly reduced the flux underestimation ( $p < 0.05$ ). Also, the use of non-linear flux calculation method significantly improved the flux estimation; however, simultaneously the uncertainty in the fluxes was increased. We provide correction factors, which can be used to correct the under- or overestimation of the fluxes by the chambers in the experiment.

© 2012 Elsevier B.V. All rights reserved.

\* Corresponding author. Tel.: +358 9 19151085; fax: +358 9 19148802.

E-mail addresses: mari.pihlatie@helsinki.fi (M.K. Pihlatie), jrc@life.ku.dk (J.R. Christiansen), hermanni.aaltonen@helsinki.fi (H. Aaltonen), janne.fj.korhonen@helsinki.fi (J.F.J. Korhonen), annika.nordbo@helsinki.fi (A. Nordbo), terhi.rasilo@helsinki.fi (T. Rasilo), giuseppe.benanti@ucdconnect.ie (G. Benanti), michael.giebels@zalf.de (M. Giebels), helmyhammad@gmail.com (M. Helmy), jatta.sheehy@mtt.fi (J. Sheehy), stephanie.jones@sruc.ac.uk (S. Jones), radjusz@up.poznan.pl (R. Juszczak), roland.klefoth@wur.nl (R. Klefoth), raquelvale@isa.utl.pt (R. Lobo-do-Vale), paulayana@gmail.com (A.P. Rosa), peter.schreiber@zmaw.de (P. Schreiber), dominique.serca@aero.obs-mip.fr (D. Serça), sara.vicca@ua.ac.be (S. Vicca), benjamin.wolf@kit.edu (B. Wolf), jukka.pumpanen@helsinki.fi (J. Pumpanen).

<sup>1</sup> Present address: Department of Forest Sciences, University of British Columbia, Vancouver, Canada.

## 1. Introduction

The static chamber method (non-flow-through-non-steady-state chamber, Livingston and Hutchinson, 1995) is the most commonly used method to measure non-reactive greenhouse gas (GHG) fluxes, especially methane ( $\text{CH}_4$ ) and nitrous oxide ( $\text{N}_2\text{O}$ ), from soils. The basic principle of this technique is to cover a known area of soil with a closed chamber that allows the gas exchange between the soil below the chamber and the chamber headspace. The gas concentration change over time inside the chamber headspace is quantified and translated into a flux rate, representing the flux into or out of the soil.

Debates on how to design an optimal chamber and how to calculate the gas fluxes from soils have been going on for more than 30 years (e.g. Anthony et al., 1995; Conen and Smith, 2000; Forbrich et al., 2010; Hutchinson and Mosier, 1981; Kroon et al., 2008; Kutzbach et al., 2007; Livingston et al., 2005, 2006; Matthias et al., 1978; Pedersen et al., 2010). Recommendations of using a fan to mix the chamber headspace (Christiansen et al., 2011; Pumpanen et al., 2004), a vent tube to minimize pressure changes in the chamber (Hutchinson and Livingston, 2001; Hutchinson and Mosier, 1981; Xu et al., 2006), and a proper insulation or construction to avoid uncontrolled leakage from the chamber (Hutchinson and Livingston, 2001) are still being discussed and are not widely adopted. The effect of chamber size and geometry on GHG fluxes has not been as widely discussed or tested, although they are key issues in assessing how well the chamber is able to detect the GHG fluxes. In addition, linear regression is the most common method to calculate chamber based  $\text{CH}_4$  and  $\text{N}_2\text{O}$  fluxes from soils, though it has been documented to lead to systematic underestimation of the fluxes (Anthony et al., 1995; Gao and Yates, 1998a; Livingston et al., 2005; Kroon et al., 2008; Kutzbach et al., 2007; Pedersen et al., 2010).

Emission measurements of greenhouse gases with closed static chambers imply that the concentration of the target gas increases in the headspace. This gas accumulation decreases the natural concentration gradient between the soil and the chamber headspace and may significantly reduce the gas efflux (Davidson et al., 2002; Kutzbach et al., 2007; Livingston and Hutchinson, 1995; Nay et al., 1994). The purpose of the flux measurement is to obtain an estimate of the undisturbed flux, the flux prior to the chamber deployment. When applying linear regression, one assumes that the gas concentration gradient between the source and the atmosphere does not change, and that the flux is constant during the entire enclosure. A non-linear function (e.g. exponential function) implicitly accounts for the decreasing efflux during the enclosure and estimates the flux at time zero of the chamber closure.

Inter-comparisons of different chamber designs in controlled conditions in combination with different flux calculation methods are scarce and the focus has been on  $\text{CO}_2$  (Butnor and Johnsen, 2004; Gao and Yates, 1998b; Nay et al., 1994; Widen and Lindroth, 2003). Pumpanen et al. (2004) performed a chamber calibration campaign for 20 different  $\text{CO}_2$  efflux chambers representing static chambers (non-flow-through-non-steady-state chamber), closed dynamic chambers (flowed-through-non-steady-state) and open dynamic chambers (flow-through-steady-state). They found that the bias of the  $\text{CO}_2$  fluxes was greatest with static chambers, which underestimated or overestimated the fluxes between  $-35$  and  $+6\%$  depending on the type of chamber, gas sampling and analysis, and the method of mixing the chamber headspace air. The largest underestimations were observed with static chambers based on syringe gas sampling, which is the most common method in the flux measurements of  $\text{CH}_4$  and  $\text{N}_2\text{O}$  fluxes.

Even though the studies with  $\text{CO}_2$  chambers have identified critical issues regarding chamber design and sampling, the results are not directly applicable to chambers used for non- $\text{CO}_2$

greenhouse gases, such as  $\text{CH}_4$  and  $\text{N}_2\text{O}$ . First of all, chamber designs and sampling protocols are often different.  $\text{CH}_4$  and  $\text{N}_2\text{O}$  are most often sampled manually in the field and subsequently analyzed off-site using gas chromatographic methods. In contrast,  $\text{CO}_2$  fluxes are typically determined *in situ* using online analyzers connected to dynamic chambers with a constant headspace mixing. Furthermore,  $\text{CO}_2$  fluxes can be several degrees of magnitude larger than  $\text{CH}_4$  and  $\text{N}_2\text{O}$  fluxes, leading to higher concentration change within chamber headspace over an enclosure, and allowing for a lower sensitivity of the gas analyzers and shorter enclosure times.

In order to minimize the errors related to the measurements of non- $\text{CO}_2$  greenhouse gas exchange, such as  $\text{CH}_4$  and  $\text{N}_2\text{O}$ , there is an urgent need to perform similar evaluation of the chambers in controlled laboratory conditions. We organized a static chamber comparison campaign to gain new knowledge on the differences between static chambers typically used to measure  $\text{CH}_4$  and  $\text{N}_2\text{O}$  fluxes from soils. Both  $\text{CH}_4$  and  $\text{N}_2\text{O}$  were measured in the experiment; however, here we report the results of  $\text{CH}_4$  only. The tested chambers differed in size, shape and material, and were originally operated in different ecosystems (peatlands, forests, agricultural fields). Christiansen et al. (2011) report the effects of chamber placement, manual sampling and headspace mixing on  $\text{CH}_4$  fluxes for two static chambers. Here we report the results of a comparison of 15 chambers, and provide general guidelines for chamber designs and flux calculation procedures.

The overall aims of the campaign were (1) to quantitatively assess the uncertainties and errors related to static chamber measurements, (2) explain uncertainties and errors by chamber design and flux calculation methods, and (3) to provide guidelines for static chamber designs, sampling procedures, and flux calculation methods.

## 2. Materials and methods

### 2.1. Calibration system

The calibration campaign took place at Hyytiälä Forestry Field Station ( $61^{\circ}51'N$ ,  $24^{\circ}17'E$ ), 152 m above sea level between 11th of August and 10th of October 2008. The calibration system was originally built for  $\text{CO}_2$  chamber calibration and is presented in detail by Pumpanen et al. (2004). A schematic presentation of the measurement setup is presented in Fig. 1.

The principle of the calibration system is to establish a controlled diffusive gas flux through a porous medium (sand bed) of a known density and porosity. The flux is created by injecting a known concentration of the target gas into a tank with defined volume and a homogenous sand bed on the top. The concentration gradient between air inside and outside the tank drives the diffusive flux from the tank through the sand bed. This flux is referred to as the reference flux in this paper. The calibration system can strictly be viewed as a non-steady-state system because the concentration in the tank decreases over time. This decrease in the concentration, however, is so small that the reference flux can be assumed as constant (see Section 4.1).

Simultaneous chamber measurements on the top of the sand bed enable direct comparison between the chamber and the reference fluxes, and allows for a subsequent quantification of the potential under- or overestimations of each tested chamber.

The calibration system consisted of a cylindrical stainless steel tank (diameter 1.13 m, height 1.0 m) with a 0.15 m thick sand bed (diameter 1.0 m) on the top. The sand was placed on top of a 0.02 m thick perforated high-density polyethylene lid, which allowed air to move freely between the sand and the tank. A porous polypropylene gauze was placed between the sand and the lid to prevent the sand from falling into the tank. Air inside the tank was

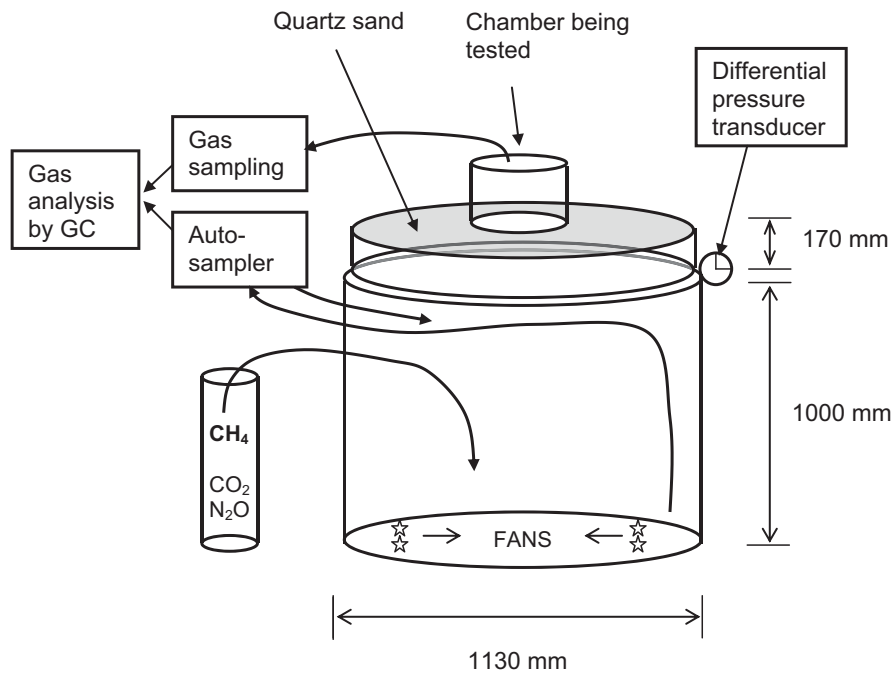


**Fig. 1.** Schematic presentation of the calibration system modified from Pumpanen et al. (2004). Gas samples from the tested chambers and calibration tank are sampled into glass vials and are analyzed off-line by a gas chromatograph. Prior to sampling into the vials, the Autosampler flushes the vials with the air from the calibration tank and returns the air back to the tank.

continuously mixed with four 12 V fans installed at the bottom of the tank during the reference gas injections. During the chamber measurements, the fan speed was reduced by setting the power supply for the fans to 6 V.

We measured the chamber fluxes from three different sands: dry fine quartz sand with particle diameter of 0.05–0.2 mm (S1), dry coarse quartz sand with particle diameter of 0.6 mm (S2), and wetted fine quartz sand (S3) by mixing sand and water in the volume ratio of 4:1. The respective air-filled porosities of the sand beds were 53%, 47% and 33%. Homogeneity of the sand water content and porosity were measured each week after the flux measurements with wet sand. This was done by sampling 5 replicate volumetric sand samples from the top of the sand bed, weighing the samples fresh and after drying them at 105 °C for 24 h.

The air temperature (pt100, model FK422, Heraeus, Hanau, Germany) and pressure differential between the tank and the atmosphere above the sand bed (Omega PX653, Omega Engineering Inc., Stamford, CT) were measured continuously at 15 second intervals using a Nokeval datalogger (Nokeval Oyj, Nokia, Finland). Air and tank temperatures and pressure differential were monitored to evaluate possible differences or changes within the calibration tank during the measurements. The air temperatures were used for correcting chamber CH<sub>4</sub> fluxes, if the chamber headspace temperatures were not available.

## 2.2. Chamber calibration protocol

The calibration procedure of each chamber for a certain concentration level followed five steps: (1) Preparation of the sand bed. (2) Installation of open chambers or collars on the sand bed. (3) Injection of the reference gas CH<sub>4</sub> into the tank with an amount corresponding to the desired flux level and stabilization of the system for a minimum of 75 min. (4) Two consecutive flux measurements with each chamber, with a 10-min break in between, and simultaneous gas sampling from the tank. (5) Preparation of the subsequent flux level, injection of the reference gases. Steps 3–5 were carried out until four flux levels had been repeated for each sand type.

During each week of the measurement campaign, one to three static chambers were calibrated. Four flux levels (FL1–FL4) were created by injecting increasing amounts (15–150 mL) of CH<sub>4</sub> (200,000 ppm CH<sub>4</sub> in N<sub>2</sub>, AGA, Finland) into the calibration tank.

## 2.3. Chamber specifications

The investigated chambers were from different research groups across Europe. They varied in size, shape, material; all except one chamber (number 9) were non-transparent, they were operated with different headspace mixing strategies (fan, syringe), and one of them included a vent-tube. Details of the chamber materials and dimensions are given in Table 1. The chambers are grouped into those without a fan (chambers 1–7) and those with a fan (chambers 8–15) to mix the headspace air. Within these groups the chamber number increases with chamber height.

In Christiansen et al. (2011) chambers 7 and 15 were referred to as 16 and 18, respectively. Chamber 12 was the same as that of NSNF-3 used for CO<sub>2</sub> calibration by Pumpanen et al. (2004).

## 2.4. Sampling protocol from chambers and calibration tank

In order to ensure a uniform protocol throughout the campaign and to produce comparable results, gas sampling from the chamber headspace and the gas chromatographic (GC) analysis for all the investigated chambers were aimed at being similar. If a chamber was equipped with a fan and/or a pressure vent-tube, these were also used in the campaign.

Two consecutive chamber enclosures were made during each flux level with a 10-min break during which the chambers were vented. All chambers were closed for 35 min in each enclosure. During the enclosure period, a total of 4–8 gas samples were taken from the chamber headspace, the first 3–5 min after the start of the closure and then at 6 or 10 min intervals per enclosure. Sampling during the first minutes of the closure was intentionally avoided due to the pressure disturbance caused by the placement of the chamber (Davidson et al., 2002; Pumpanen et al., 2009;

**Table 1**  
The numbering of the chambers, the week of the year when each chamber was calibrated, participant, and dimensions, collar insertion depth, information on headspace mixing and vent-tube, and number of gas samples per closure of the static chambers tested during the calibration campaign.

ID	Participant	Institute of the participant	Chamber shape	Chamber, collar material <sup>a</sup>	Base diameter or side (m)	Basal area (m <sup>2</sup> )	Height (m)	Volume (m <sup>3</sup> )	Collar insertion depth (m)	Fan	Vent tube	Samples/closure
1	Stephanie Jones	Scottish Agricultural College, CEH	Round	PP, PVC	0.40	0.13	0.15	0.019	0.05	No	No	6
2	Raquel Lobo-do-Vale	ISA, Universidade Técnica de Lisboa	Round	PVC	0.30	0.07	0.15	0.011	0.10	No	No	4
3	Roland Klefoth	Wageningen, UR	Round	PE	0.20	0.03	0.17	0.005	0.05	No	No	4
4	Mohamed Helmy	University College Dublin	Rectangular	SS, SS	0.40 × 0.40	0.16	0.18	0.029	0.07	No	No	4
5	Ana Paula Rosa	Centro de Ecologia e Biologia Vegetal	Round	PVC, PVC	0.30	0.08	0.23	0.017	0.07	No	No	6
6	Giuseppe Benanti	University College Dublin	Rectangular	S	0.51 × 0.51	0.26	0.24	0.062	0.06	No	No	4
7	Radoslaw Juszcak	Poznan University of Life Sciences	Round	PVC	0.5 <sup>b</sup>	0.20	0.41	0.068	0.05	No	No	6
8	Sara Vicca	University of Antwerp	Round	PVC	0.10	0.01	0.14	0.002	0.05	Yes <sup>c</sup>	No	6
9	Benjamin Wolf	Institute for Meteorology and Climate Research (IMK-IFU)	Rectangular	S, PMMA	0.50 × 0.50	0.25	0.15	0.038	0.10	Yes	No	6
10	Local organizers	University of Helsinki	Round	Zn–Sn	0.31	0.08	0.20	0.015	0.06	Yes	No	6
11	Local organizers	University of Helsinki	Round	Zn–Sn	0.31	0.08	0.27	0.021	0.08	Yes	No	4
12	Local organizers	University of Helsinki	Round	Polycarbonate	0.22	0.04	0.30	0.009	0.02	Yes	No	6
13	Peter Schreiber	University of Greifswald	Rectangular	Al, SS	0.60 × 0.60	0.36	0.35	0.127	0.12	Yes	Yes <sup>d</sup>	8
14	Jatta Sheehy	MTT Agrifood Research Finland	Rectangular	Al, SS	0.60 × 0.60	0.36	0.49	0.176	0.04	Yes	No	6
15	Michael Giebels	Institute for Landscape Biogeochemistry	Round	PVC	0.50 <sup>b</sup>	0.20	1.82	0.195	0.05	Yes	No	6

<sup>a</sup> PVC, poly vinyl chloride; SS, stainless steel; S, steel; PE, polyethylene; PMMA, polymethyl methacrylate (Pexiglas); Zn–Sn, zink coated tin (galvanized tin).

<sup>b</sup> Chamber decreases in diameter towards the top of the chamber.

<sup>c</sup> Chamber headspace was mixed with a pump circulating the air between the headspace and a 1.1 L bottle to increase the headspace volume (Vicca et al., 2009).

<sup>d</sup> Vent-tube dimensions: length 0.55 m, inner diameter 0.012 m.

Christiansen et al., 2011), and in order to have enough time for preparing the manual sampling.

Gas samples were taken from one point of the chamber headspace with polypropylene syringes (BD Plastipak), 100 mL (20 mL only for chambers 1, 2 and 10) in volume, and immediately transferred into glass vials (12 mL Soda glass Labco Exetainer<sup>®</sup>, Labco Limited, UK). To minimize the pressure disturbance of the gas sampling, we used smaller syringes (20 mL) and pre-evacuated glass vials in chambers 1, 2 and 10. For the rest of the chambers, the glass vials were flushed with compressed air prior to the gas injection. During the headspace sampling, the syringe was flushed three times with chamber headspace air by always emptying the syringe into the chamber headspace. The fourth flush was transferred to the vial. The vials were first flushed with 85 mL of the sample air, and pressurized with the remaining 15 mL. The pre-evacuated vials were directly pressurized with the full syringe volume of 20 mL. Thus, all vials were pressurized to approximately +2400 mbar. The overpressure facilitated the transfer of the sample from the vial to the gas chromatograph.

During the chamber measurements, gas samples from inside the calibration tank were automatically taken by a custom made autosampler (MaSa, Pohja-metallityöpaja, Juupajoki, Finland), and injected into the glass vials (12 mL Soda glass Labco Exetainer<sup>®</sup>, Labco Limited, UK). The gas samples were taken at 5-min intervals during the two replicate chamber measurements of 35 min. The autosampler flushed the vial for 1 min with the tank air using a double-needle in a closed circuit with the tank. Following the flushing, the second needle was lifted up and the vial was pressurized to +2400 mbar with tank air. The degree of pressurization in vials with tank air was regularly checked with a pressure sensor (Tensimeter, Soil Measurement Systems, Arizona, USA). All the gas samples were stored in dark at +4 °C for a maximum of one month.

## 2.5. Gas analysis

Gas samples from the chambers and the calibration tank were analyzed for CH<sub>4</sub> with an Agilent Gas Chromatograph (model 7890A, Agilent Technologies, USA) using a Flame Ionization Detector (FID). Helium was used as a carrier gas with a flow rate of 45 mL min<sup>-1</sup>, and synthetic air (450 mL min<sup>-1</sup>) and hydrogen (H<sub>2</sub>, 45 mL min<sup>-1</sup>) were used for the flame gases and nitrogen (N<sub>2</sub>, 5 mL min<sup>-1</sup>) as a make-up gas for the FID. Oven and the detector temperatures were 60 °C and 300 °C, respectively. The gas chromatograph (GC) was connected to an autosampler (Gilson GX-271 Liquid Handler) fitting 220 vials to allow for an automatic injection of the gas samples into the GC.

Separate calibration methods were used for small and high gas concentrations from the measurement campaign. All the samples from the chambers and from the calibration tank at flux levels 1–2 were analyzed using a six-point standard curve with concentrations between 1.68 and 10.80 ppm for CH<sub>4</sub>. Gas samples from the calibration tank at flux levels 3–4 were run using a six-point standard curve with concentrations between 10.80 and 30.60 ppm CH<sub>4</sub>. The standards were analyzed at the beginning and after every 100 gas samples. ChemStation B.03.02 software was used to calculate the concentrations in the gas samples.

We estimated the method quantification limit (MQL) for the gas chromatograph on standards ( $N = 10$ ) of CH<sub>4</sub> (2.200 ppm). The MQL represents the lowest concentration that can accurately be measured for the method used in the GC setup (Corley, 2003). The MQL was calculated as (Corley, 2003)

$$\text{MQL} = 3 \text{MDL} = 3t_{99\%}S_{\text{dev}}, \quad (1)$$

where  $t_{99\%}$  is the students  $t$ -value at the 99% confidence interval (3.250) with  $N - 1$  degrees of freedom and  $S_{\text{dev}}$  is the standard deviation of the concentration measurements.  $\text{MQL}_{\text{CH}_4} = 0.16 \text{ ppm}$ .

Further, we estimated detection limits of the chamber and reference gas fluxes based on the MQL of the GC. We calculated a minimum detectable flux from the tested chambers (linear regression) or the calibration tank (exponential fit) by assuming a minimum increase of 0.16 ppm CH<sub>4</sub> concentration within chamber headspace during one chamber enclosure of 35 min, or a minimum decrease of 0.16 ppm CH<sub>4</sub> within the calibration tank during one measurement cycle of 75 min. The resulting detection limits for the chambers ranged from 28.3 to 176  $\mu\text{g CH}_4 \text{ m}^{-2} \text{ h}^{-1}$  for the shallowest (and smallest volume) chamber 2 and the tallest chamber 15, respectively. The corresponding mean detection limit for the reference fluxes ( $\pm S_{\text{dev}}$  of S1, S2, S3) was  $122 \pm 1.7 \mu\text{g CH}_4 \text{ m}^{-2} \text{ h}^{-1}$ .

## 2.6. Flux calculations

### 2.6.1. Reference fluxes

The reference flux was calculated by fitting an exponential function using the least squares method to the measured tank concentration data. The fitting was done over a period of a full flux level (75–80 min,  $N = 17$ ) during which two replicate chamber measurements were made. The exponential function has the form (Pumpanen et al., 2004)

$$C(t) = C_{\infty}e^{(-\alpha t)}, \quad (2)$$

where  $C(t)$  is the fitted CH<sub>4</sub> concentration inside the calibration tank (ppm),  $C_{\infty}$  is the measured concentration in the calibration tank at the beginning of the measurement period (ppm),  $t$  is the time (s) and  $\alpha$  is the concentration decline rate (s<sup>-1</sup>). Using the fitted tank concentrations of CH<sub>4</sub>, the reference flux ( $F$ , ppm m s<sup>-1</sup>) was then estimated for each time step of the autosampler (5 min) using a time discrete exponential function (Pumpanen et al., 2004)

$$F_{\text{ppm}} = \frac{V(C(t_1) - C(t_2)) + V_s((C(t_1) + C_0(t_1))/2 - (C(t_2) + C_0(t_2))/2)}{(t_2 - t_1)A}, \quad (3)$$

where  $C_0(t_i)$  is the ambient CH<sub>4</sub> concentration at time  $t_i$ ,  $V$  is the volume of the calibration tank (1 m<sup>3</sup>),  $V_s$  is the volume of air-filled porosity in the sand (0.061, 0.054 and 0.038 m<sup>3</sup> for S1, S2 and S3, respectively), and  $A$  is the surface area of the sand bed (0.77 m<sup>2</sup>). The change in the CH<sub>4</sub> concentration in  $V_s$  was taken into account by assuming the concentration in the sand to be an average of  $C$  and  $C_0$ . Assuming that  $C_0$  was constant (1.9 ppm), the flux (ppm m s<sup>-1</sup>) was calculated based only on the change in CH<sub>4</sub> concentration within the tank

$$F_{\text{ppm}} = \frac{V(C(t_1) - C(t_2)) + V_s((C(t_1) - C(t_2))/2)}{(t_2 - t_1)A}. \quad (4)$$

Finally, the flux ( $F$ ) in  $\mu\text{g CH}_4 \text{ m}^{-2} \text{ h}^{-1}$  was calculated using the molecular mass of CH<sub>4</sub> ( $M$ , 16.042 g mol<sup>-1</sup>), ideal gas mole volume ( $V_m$ , 0.0224 m<sup>3</sup> mol<sup>-1</sup>) and mean ambient air temperature above the calibration tank ( $T$ , °C)

$$F = F_{\text{ppm}} \frac{M}{V_m} \frac{273.16}{273.16 + T} 3600. \quad (5)$$

When the reference flux and a simultaneously measured chamber flux were compared, the reference flux at the time of the chamber enclosure was used, resulting in two replicate reference fluxes within the full flux level period.

Reference fluxes were filtered by discarding those time series of CH<sub>4</sub> concentrations displaying unnatural scatter between the measurement points. This occurred mostly with the smallest flux level, and resulted from measuring concentrations close to the detection limit of the GC system. The rest of the discarded measurements were attributed to errors originating from gas sampling, vial storage, leakage of vials or gas analysis. This filtering removed 15% of the reference flux calculations.

### 2.6.2. Chamber fluxes

Fluxes of CH<sub>4</sub> to the chambers were calculated by a linear and a non-linear (exponential) regression using a MatLab-R2010a script (The MathWorks Inc., Natick, MA, USA).

The final flux value ( $F_0$ ) at the time of chamber closure ( $t=0$ ) in  $\mu\text{g CH}_4 \text{ m}^{-2} \text{ h}^{-1}$  is

$$F_0 = S \frac{V}{A} \frac{M}{V_m} \frac{273.16}{273.16 + T} 3600, \quad (6)$$

where  $S$  is the slope or time derivative of the linear ( $S_{\text{lin}}$ ) or exponential ( $S_{\text{exp}}$ ) fit ( $\text{ppm s}^{-1}$ ) at chamber closure,  $V$  chamber volume ( $\text{m}^3$ ),  $A$  chamber area ( $\text{m}^2$ ),  $M$  molecular mass of CH<sub>4</sub> ( $16.042 \text{ g mol}^{-1}$ ),  $V_m$  ideal gas mole volume ( $0.0224 \text{ m}^3 \text{ mol}^{-1}$ ) and  $T$  chamber headspace temperature ( $^{\circ}\text{C}$ ).

The linear development of the chamber headspace concentration ( $C$ , ppm) as a function of time ( $t$ , s) can be described as

$$C(t) = C_0 + F_0 \frac{t}{h}, \quad (7)$$

where  $C_0$  is the gas concentration at closure,  $F_0$  is the constant flux ( $\text{ppm m s}^{-1}$ ),  $h = V/A$  the effective chamber height (m), and the time derivative (slope) at closure ( $\text{ppm s}^{-1}$ ) is

$$S_{\text{lin}} = \frac{F_0}{h}. \quad (8)$$

The exponential development of chamber CH<sub>4</sub> concentration can be described (Hutchinson and Mosier, 1981; Pedersen et al., 2010) as

$$C(t) = C_{\infty} + (C_0 - C_{\infty})e^{-\kappa t}, \quad (9)$$

where  $C_{\infty}$  is the assumed constant concentration source at a depth  $Z$  (m) below the soil surface. In our experiment,  $C_{\infty}$  was the tank gas concentration at the beginning of the measurements, which also equals to the concentration that the chamber headspace approaches with time, and  $\kappa$  is the concentration saturation rate ( $\text{s}^{-1}$ ). The time derivative (slope) at chamber closure ( $\text{ppm s}^{-1}$ ) is

$$S_{\text{exp}} = (C_{\infty} - C_0)\kappa. \quad (10)$$

Note that the linear fit has two unknown fitting parameters ( $C_0$  and  $F_0$ ) whereas the exponential fit has three ( $C_0$ ,  $C_{\infty}$  and  $\kappa$ ) and thus the exponential fit is more prone to errors when there are only a few measurement points per closure.

Chamber fluxes were filtered using a goodness-of-fit parameter, namely, normalized root-mean-square-error (NRMSE) (Christiansen et al., 2011). The NRMSE is the root-mean-square-error of the fit divided by the range (max–min) of gas concentrations during the enclosure. Hence, NRMSE is a relative measure of the distances of individual measurement points from the fit. We filtered outliers from the data using NRMSE limits, which were defined based on Boxplot statistics in PASW Statistics 18 program (IBM corporation, Somers, NY, United States). The smallest flux level (FL1) had generally higher NRMSE values (median 0.02) as compared to the NRMSE of FL2–FL4 (median 0.01). The resulting NRMSE limits below which the data were accepted equalled approximately to the 75th percentiles of the data in each flux level, and were 4% (FL1), 2% (FL2), 2% (FL3) and 2% (FL4), respectively. In order to compare the linear and exponential flux calculation methods, we ran the NRMSE filtering for the exponential fits only and thereafter removed the same chamber enclosures in the linear calculations. The final accepted data hence included the same number of enclosures for both flux calculation methods. This filtering removed 7, 10, 7 and 13% of the closures in flux levels 1, 2, 3 and 4, respectively. In addition, three exponential chamber fluxes with a negative flux sign were manually removed. In total, 9% of all the chamber closures were filtered out.

### 2.7. Comparison of chamber and reference fluxes

The specific over- or underestimation for a given flux level and chamber was calculated as the ratio of the flux and the reference flux. To obtain a general estimate of the over- or underestimations of each chamber over all four flux levels, we calculated a linear regression between the reference fluxes and the chamber fluxes (linear and exponential) across all four flux levels (see Fig. A1). The chamber performances were evaluated separately for each sand type. The regression line was forced through origin assuming that at a zero reference flux the chamber flux should also be equal to zero. The slope of the regression line then indicated whether the chamber over- or underestimated the reference fluxes at these four flux levels. The slope of each chamber was then converted to a correction factor, which is defined as  $1/\text{slope}$  (Tables 3 and A1). The corrected chamber flux could then be obtained by multiplying the measured chamber flux by the correction factor. A correction factor was not calculated for those chambers and sand types when there were measurements only from two or less flux levels. These data points are still visible in Fig. A1. Comparison of the confidence intervals of the correction factors of individual chambers to the confidence intervals of the reference fluxes shows which of the under- or overestimations are statistically significant (Table A1).

### 2.8. Statistical analysis

Statistical differences between the chamber and the reference fluxes in different treatments were tested using PASW Statistics 18 program (IBM corporation, Somers, NY, United States) with a significance accepted at  $p < 0.05$ . At first, the normality and the equality of variances of the test parameters were tested using Kolmogorov–Smirnov test and Levene's test, respectively. The requirements of normal distribution and equal error variances were not met with most of the parameters. Hence, the non-parametric Kruskal–Wallis test was used to test whether there were significant differences in the reference fluxes ( $F_{\text{ref}}$ ), chamber fluxes ( $F_{\text{lin}}$ ,  $F_{\text{exp}}$ ) or the ratios of chamber to reference fluxes ( $R_{\text{lin}}$ ,  $R_{\text{exp}}$ ) between the treatments (sand types (S), flux levels (FL), chamber height ( $h$ ), basal area ( $A$ ), volume ( $V$ ), collar insertion depth, or number of gas samples per closure). Wilcoxon signed rank test was used to test whether the fitting parameter NRMSE differed between  $F_{\text{lin}}$  and  $F_{\text{exp}}$ , and, a one-sample  $T$ -test was used to test if  $R_{\text{lin}}$  or  $R_{\text{exp}}$  were significantly different from one.

Kendall's tau  $b$  correlation matrix was used to test for significant (2-tailed) correlations between the parameters  $R_{\text{lin}}$ ,  $R_{\text{exp}}$ ,  $h$ ,  $A$ ,  $V$ , collar insertion depth, and number of gas samples per closure. To evaluate the importance of individual correlated parameter, partial correlations were calculated using the Kendall's tau  $b$  correlation coefficients by fixing each of the three correlated parameters at a time as

$$r_{12.3} = \frac{r_{12} - r_{13}r_{23}}{\sqrt{(1 - r_{13}^2)(1 - r_{23}^2)}}, \quad (11)$$

where  $r_{12.3}$  is the correlation between parameters 1 and 2 when the parameter 3 is fixed,  $r_{12}$  is the correlation between parameters 1 and 2,  $r_{13}$  is the correlation between parameters 1 and 3, and  $r_{23}$  is the correlation between parameters 2 and 3.

## 3. Results

### 3.1. Performance of the calibration system

The flux measurements between different weeks of the campaign were repeatable. The variation in the measured CH<sub>4</sub> concentrations and in the measured reference fluxes between the different weeks was small (Fig. 2). The standard error of the

**Table 2**  
CH<sub>4</sub> concentrations in the ambient air and inside the calibration tank at the start of the measurements and the measured reference CH<sub>4</sub> fluxes for the four flux levels (FL1–FL4) and three sand types.

Sand type	Flux level	Ambient concentration (ppm)	Measured tank concentration (ppm)	[95% confidence interval]	Measured reference flux ( $\mu\text{g m}^{-2} \text{h}^{-1}$ )	[95% confidence interval]
Fine dry (S1)	1	1.9	4.9	[4.8–4.9]	230	[215–244]
	2	1.9	9.6	[9.2–9.9]	647	[599–694]
	3	1.9	14.4	[14.1–14.7]	1025	[985–1065]
	4	1.9	27.8	[26.9–28.6]	2113	[2058–2169]
Coarse dry (S2)	1	1.9	5.0	[4.8–5.1]	228	[207–249]
	2	1.9	9.8	[9.6–10.0]	606	[560–651]
	3	1.9	15.2	[14.6–15.8]	1023	[969–1078]
	4	1.9	28.8	[27.9–29.7]	2168	[2071–2265]
Fine wet (S3)	1	1.9	4.9	[4.8–5.1]	206	[169–243]
	2	1.9	9.9	[9.7–10.1]	381	[465–496]
	3	1.9	15.7	[15.3–16.1]	823	[763–883]
	4	1.9	34.1	[33.1–35.1]	2003	[1616–2390]

reference fluxes over all weeks, flux levels and sand types was on average 5% of the measured reference fluxes.

The reference fluxes ( $F_{\text{ref}}$ ) across all four flux levels differed between the sand types ( $p=0.006$ ) (Fig. 2 and Table 2). The fluxes measured in the fine wet sand (S3) were on average 13% smaller than the fluxes in fine dry sand (S1) and coarse dry sand (S2) (Fig. 1). The reference fluxes between S1 and S2 did not differ from each other.

We estimated that, during a chamber enclosure the reference flux decreased by 4% at maximum. This decrease was highest with the highest flux level and biggest soil porosity (S1). We assume that this decrease in the reference flux represents the maximum deviation of the measured reference flux from a constant steady-state reference flux.

### 3.2. Chamber fluxes

#### 3.2.1. Chamber design specific over- or underestimations

The fluxes measured by different chambers showed large variations in relation to the reference fluxes. There was a group of chambers that tended to underestimate the reference fluxes systematically both with linear and exponential calculation methods (chamber numbers 3, 5, 8, 10 and 11) (Figs. 3 and A1). The highest underestimations of individual chamber fluxes were measured on

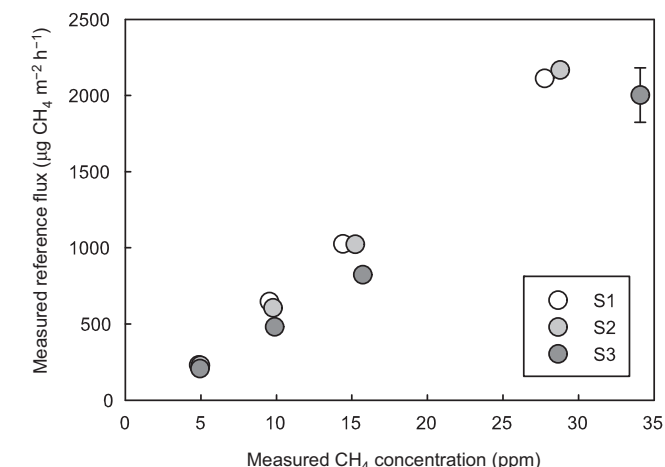


**Fig. 2.** Measured reference fluxes of CH<sub>4</sub> against measured CH<sub>4</sub> concentrations inside the calibration tank at the start of each chamber measurement during the whole measurement campaign. Colors represent concentrations for dry fine sand (S1), dry coarse sand (S2) and fine wet sand (S3). Bars denote standard errors of the mean. Note that the bars of the measured CH<sub>4</sub> concentration are too small to be visible.

fine dry sand (S1). Another group of chambers tended to underestimate the fluxes with the linear regression method, but resulted in fluxes close to or above the reference flux with the exponential flux calculation method. Chamber 15 tended to regularly overestimate the reference fluxes with both the linear and exponential flux calculation methods (Fig. 3 and Table A1).

The ratio of linear chamber fluxes to the reference fluxes ( $R_{\text{lin}}$ ) correlated positively with chamber height ( $r=0.24$ ,  $p<0.001$ ), chamber area ( $r=0.45$ ,  $p<0.001$ ), chamber volume ( $r=0.50$ ,  $p<0.001$ ) and the number of gas samples per enclosure ( $r=0.14$ ,  $p=0.003$ ). The ratio of exponential chamber fluxes to the reference fluxes ( $R_{\text{exp}}$ ) correlated positively with chamber height ( $r=0.11$ ,  $p=0.006$ ), chamber area ( $r=0.27$ ,  $p<0.001$ ), chamber volume ( $r=0.29$ ,  $p<0.001$ ) and the number of gas samples per enclosure ( $r=0.14$ ,  $p=0.004$ ).  $R_{\text{lin}}$  and  $R_{\text{exp}}$  did not differ significantly between chambers with or without a fan. Partial correlations showed that the most important parameter correlating with  $R_{\text{lin}}$  and  $R_{\text{exp}}$  were chamber area and volume. The correlation of  $R_{\text{lin}}$  and chamber height disappeared when the correlation with area or volume were fixed.

Correction factors for groups of chambers based on height, basal area and volume are presented in Table 3. No matter how the chambers were grouped they always underestimated the reference fluxes with the linear regression method, as indicated by 95% confidence intervals greater than 1, whereas only the smallest chambers ( $h \leq 0.22$  m,  $A \leq 0.1$  m<sup>2</sup> and  $V \leq 0.015$  m<sup>3</sup>) underestimated the fluxes with the exponential flux calculation method (Table 3). Comparison of the correction factors and their 95% confidence intervals of individual chambers to the corresponding confidence intervals of the reference fluxes are presented in Table A1.

#### 3.2.2. The effect of sand type and flux level on chamber fluxes

The mean ratio  $R_{\text{exp}}$  ( $p=0.010$ ) and the chamber fluxes  $F_{\text{lin}}$  ( $p=0.048$ ) and  $F_{\text{exp}}$  ( $p=0.009$ ) were significantly different between the fine wet sand (S3) and the two dry sands (S1 and S2), all of the variables being always smaller with S3 compared to S1 and S2. There were no significant differences in the  $R_{\text{lin}}$  between the three sand types.

The mean ratios  $R_{\text{lin}}$  and  $R_{\text{exp}}$  of all chambers and all three sand types were nearly constant through the four flux levels (Fig. 4). Also,  $R_{\text{lin}}$  ( $p=0.99$ ) and  $R_{\text{exp}}$  ( $p=0.90$ ) were not significantly different between the four flux levels. Indicated by the larger error bars of  $R_{\text{exp}}$ , there was more variability in the first flux level between the sand types than in the flux levels FL2 to FL4 (Fig. 4). The exponential flux calculation method occasionally resulted in overestimations in this low flux level for the dry fine sand (S1) with highest soil porosity (data not shown).

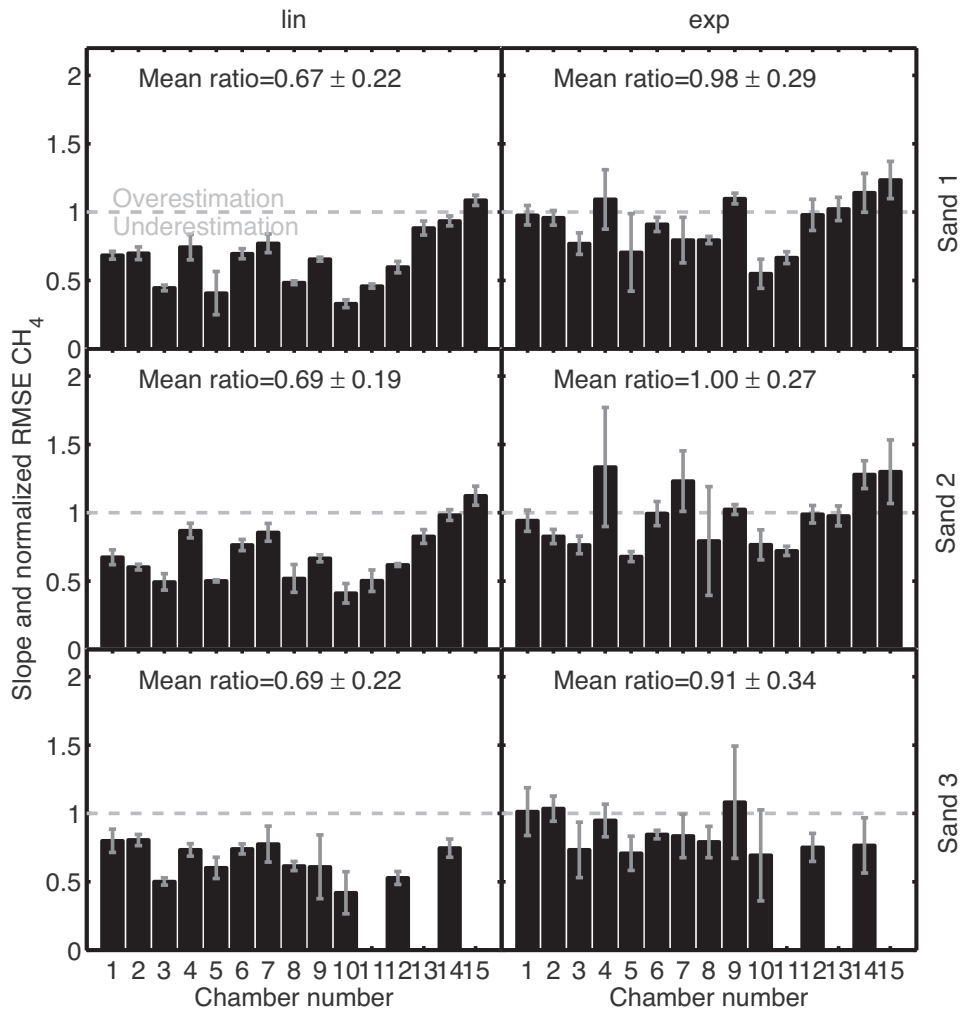


**Fig. 3.** Slopes for each chamber based on a linear fit between the chamber fluxes against the reference fluxes over the four flux levels. The slope presents the inverse of the correction factor. Error bars represent the root mean square error (RMSE) of the linear fit normalized by the mean reference flux. Mean ratio is the mean of the ratio between chamber and reference fluxes  $\pm$  standard deviation. Bars are not shown if the number of measurement points is two or less. Panels on the left show the chamber flux calculations based on a linear fit (lin) and panels on the right flux calculations based on an exponential fit (exp). Panels from the top to the bottom show the slopes measured with different sand types (Sand 1, Sand 2, Sand 3). Numbers 1–7 represent chambers without fan mixing, and numbers 8–15 chambers with a fan.

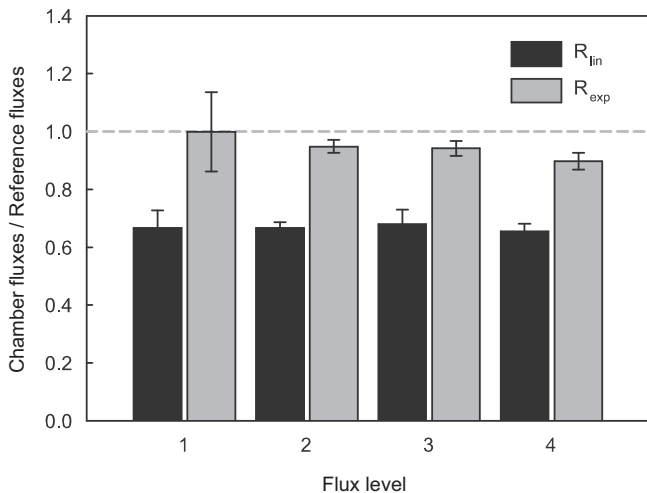


**Fig. 4.** Relation of mean chamber fluxes to mean reference fluxes for four different flux levels. All 15 chambers and 3 sand types are included and values are given for fluxes calculated by the linear ( $R_{lin}$ ) and exponential ( $R_{exp}$ ) flux calculation methods. On the Y-axis the value 1 represents the value where chamber fluxes equal the reference fluxes (no under- or overestimation). Error bars represent standard errors of the means.

3.2.3. The effect of flux calculation method on chamber fluxes

The linear regression method resulted in underestimation of the chamber fluxes, whereas the exponential regression showed both under- and overestimations of the fluxes (Fig. 3). The mean slope (inverse of the correction factor) for the linear flux calculation method was 0.67 (range 0.33–1.12), and that for the exponential flux calculation method was 0.92 (range 0.55–1.33). Also,  $R_{lin}$  was significantly different from one ( $p < 0.001$ ), whereas the  $R_{exp}$  did not differ from one. The fitting parameter normalized root-mean-square-error (NRMSE) was significantly higher for  $F_{lin}$  as compared to NRMSE of  $F_{exp}$  ( $p < 0.001$ ).

4. Discussion

4.1. Errors and uncertainty originating from chamber design

We found clear differences in flux estimates between chambers that differed in size (height, area, volume). Also, as the ratio of chamber fluxes to the reference fluxes ( $R_{lin}$  and  $R_{exp}$ ) were not different between the chambers with or without a fan, we could further focus on evaluating the effect of chamber size on under- or overestimation. We found that the  $R_{lin}$  and  $R_{exp}$  correlated positively with chamber height ( $h$ ), area ( $A$ ) and volume ( $V$ ), indicating



**Table 3**  
Mean correction factors (1/slope) of chamber fluxes and their 95% confidence intervals for chambers divided into two size classes based on chamber height, area and volume, and a mean for all the chambers (1–15) for a linear and exponential calculation method for three sand types (S1, S2, S3).

Chamber group	Fine dry sand (S1)			Coarse dry sand (S2)			Fine wet sand (S3)					
	Linear	95% confidence interval	Exponential	95% confidence interval	Linear	95% confidence interval	Exponential	95% confidence interval	Linear	95% confidence interval	Exponential	95% confidence interval
$h \leq 0.22$ m (n=9)	1.83	1.67–1.99	1.18	1.07–1.32	1.72	1.59–1.87	1.15	1.00–1.34	1.57	1.43–1.74	1.14	0.98–1.36
$h > 0.22$ m (n=6)	1.21	1.15–1.27	0.99	0.89–1.10	1.16	1.09–1.24	0.89	0.77–1.04	1.43	1.30–1.60	1.25	1.09–1.47
$A \leq 0.1$ m <sup>2</sup> (n=7)	2.05	1.91–2.21	1.29	1.17–1.43	1.92	1.76–2.11	1.26	1.14–1.42	1.73	1.57–1.92	1.27	1.08–1.55
$A > 0.1$ m <sup>2</sup> (n=8)	1.24	1.17–1.31	0.97	0.87–1.08	1.18	1.11–1.26	0.88	0.76–1.05	1.36	1.24–1.51	1.09	0.96–1.27
$V \leq 0.015$ m <sup>3</sup> (n=6)	2.03	1.88–2.20	1.26	1.14–1.40	1.91	1.79–2.04	1.24	1.11–1.41	1.73	1.54–1.92	1.27	1.08–1.55
$V > 0.015$ m <sup>3</sup> (n=9)	1.30	1.23–1.38	1.01	0.91–1.13	1.24	1.15–1.34	0.92	0.79–1.09	1.36	1.24–1.51	1.09	0.96–1.27
All (n=15)	1.52	1.43–1.62	1.10	0.99–1.22	1.44	1.34–1.55	1.03	0.90–1.20	1.52	1.38–1.69	1.18	1.02–1.40

that the flux underestimation decreased with increasing chamber size. Partial correlations revealed that when the correlation of each of these variables was fixed at a time, the most important factors influencing  $R_{lin}$  and  $R_{exp}$  were chamber area and volume.

Matthias et al. (1978) demonstrated that enclosures with small volume to basal area ratios exhibit faster concentration increases, and thus more rapid feedback to the concentration gradient, and further to the diffusive flux from the soil. To minimize these chamber effects, Livingston and Hutchinson (1995) recommended that chamber  $V$  to  $A$  ratio should be small enough to be able to quantify the concentration change; however, large enough to minimize the disturbances of the enclosure. Our observation of the flux underestimation with a wide range of chamber sizes demonstrates that most of the tested chambers disturbed the diffusive flux from the soil to the atmosphere.

We found no specific chamber size classes dividing the chambers into those that always underestimated the fluxes and those that did not. However, the small chambers ( $h \leq 0.22$  m,  $A \leq 0.10$  m<sup>2</sup> and  $V \leq 0.015$  m<sup>3</sup>) tended to underestimate the fluxes irrespective of the flux calculation method, and when the chambers were big enough ( $h > 0.22$  m,  $A > 0.10$  m<sup>2</sup> and  $V > 0.015$  m<sup>3</sup>) the fluxes were underestimated only with the linear flux calculation method. This underestimation with the linear flux calculation method decreased with increasing chamber size, especially when the chamber  $h > 0.3$  m. Hence, our measurements demonstrate that the negative “chamber effects” and the resulting flux underestimation can be minimized by increasing the size of the chamber. Similarly, Venterea and Baker (2008) suggested that irrespective of the flux calculation method, the accuracy in the flux estimation can be improved by larger chamber heights, but also by shorter deployment times, which both decrease the chamber effects.

Factors increasing the uncertainties in the flux estimation may also include problems in the gas analysis, sampling, sample storage or chamber operation (e.g. Christiansen et al., 2011; Hutchinson and Livingston, 2001; Levy et al., 2011; Rochette and Eriksen-Hamel, 2008). We found that a few chambers exhibited rather high underestimations of the fluxes with both linear and exponential flux calculation methods. For chambers 10 and 11, part of this underestimation may be explained by the fact that the insulation rubber between the collar and the chamber was presumably not gas-tight. Hence, the measured increases in the concentrations within the chamber headspace were probably lower than those that would have been there without a leak, leading to uncontrollable errors. As Hutchinson and Livingston (2001) concluded, a leakage through the seal is not controllable and creates therefore an unknown source of error.

Conen and Smith (2000) suggested that underestimations of the fluxes by static chambers can also stem from storage of the target gas within the soil underneath the chamber and not emitted into the chamber. They found that the fluxes based on the linear regression method were underestimated by up to 28% due to this storage effect. Based on the correction equation Conen and Smith (2000) provide, we estimated the proportion of CH<sub>4</sub> flux that was not emitted to the chamber headspace to be on average 7% (1–13%) in our experiment. This proportion increased with decreasing chamber volume, being highest for the smallest chambers measured on the highest soil porosity (S1). This is in line with the general result of the study, that smaller chambers exhibited the largest degree of underestimation.

#### 4.2. Errors and uncertainty originating from flux calculation method

Our results showed that the linear regression method leads to underestimation of the CH<sub>4</sub> fluxes, whereas the non-linear, exponential, flux calculation method did not show significant flux

underestimations but with few chambers lead to marked overestimations, and increased the uncertainty in the flux estimates.

We showed that the CH<sub>4</sub> concentration development within chamber headspace during the 35-min enclosure time was mostly non-linear, indicated by the higher normalized root-mean-square-error (NRMSE) of the linear fits as compared to the NRMSE of the exponential fits. The exponential fit hence better captured the concentration development within chamber headspace, indicating that the flux decreased during the chamber closure, and therefore the use of the linear regression method leads to systematic underestimations of the fluxes.

Although, as we showed, the use of non-linear flux calculation method improves the flux estimation, it is often also associated with an increased uncertainty in the flux estimate (Venterea et al., 2009). In ecosystems with low flux rates, the signal-to-noise ratio of the concentration measurements can be low. In these situations the use of an exponential model can be more vulnerable to biased flux estimates compared to the linear approach (e.g. Forbrich et al., 2010). In our experiment the two tallest chambers (14 and 15) occasionally overestimated the CH<sub>4</sub> fluxes, especially with the exponential flux calculation method. We consider that these overestimations can partly be explained by the increased uncertainty in the flux estimates due to measuring fluxes close to the detection limit.

The first minutes of the closure are the most crucial in order to model the concentration development correctly since the start of the closure defines the slope of the non-linear fit (e.g. Forbrich et al., 2010; Kroon et al., 2008; Kutzbach et al., 2007). These first minutes are also most vulnerable to disturbance due to chamber placement (Christiansen et al., 2011; Davidson et al., 2002; Lai et al., 2012), hence underlining the sensitivity of the non-linear approach. In the future the use of fast response automatic analyzers for CH<sub>4</sub> may improve the flux estimation enormously as the analyzers tend to be more sensitive than gas chromatographs and the number of gas samples per closure is not anymore a limiting factor when choosing the flux calculation method. Also, freely available scripts to calculate fluxes and analyze static chamber data (e.g. <http://cran.r-project.org/web/packages/HMR/> by Pedersen et al., 2010) have made the non-linear approaches more user-friendly and can help in analysing data even with small sample sizes.

4.3. Uncertainties and limitations of the experimental setup

Overall, based on the good between-weeks repeatability of the CH<sub>4</sub> concentrations within the calibration tank, we are confident that the measurements conducted in different weeks by different chambers are comparable. A similar conclusion was reached by Pumpanen et al. (2004) who used the same system.

The placement of a chamber may (1) alter the concentration gradient within the sand, and (2) lead to horizontal transport that may introduce a systematic underestimation of the flux out of the soil (e.g. Conen and Smith, 2000; Kutzbach et al., 2007; Pedersen et al., 2010). Firstly, we did not measure the CH<sub>4</sub> concentration within the sand but we consistently observed that the placement of chamber on the sand surface did not affect the tank concentration of CH<sub>4</sub>. Furthermore, the estimated transport time through the 0.15 m sand bed is ~63 min, making the 35-min enclosures too short a period to effectively disturb the transport out of the tank. This was tested with repeated chamber measurements with CO<sub>2</sub> chambers after injecting CO<sub>2</sub> gas in the calibration tank in the previous calibration campaign by Pumpanen et al. (2004).

These findings support the basic assumption that the diffusive flux out of the tank remains unaffected by chamber coverage and secondly that the transport can be assumed vertical in the sand bed. We cannot dismiss the possibility of horizontal transport of gas in the sand bed (Kutzbach et al., 2007; Pedersen et al., 2010). However,

**Table A1** Correction factors (1/slope) of fluxes and their 95% confidence intervals of each chamber for linear and exponential calculation method for three sand types (S1, S2, S3), and the corresponding reference fluxes scaled to the correction factors and their 95% confidence intervals.

Chamber	Fine dry sand (S1)			Coarse dry sand (S2)			Fine wet sand (S3)					
	Linear	95% confidence interval	Exponential	95% confidence interval	Linear	95% confidence interval	Exponential	95% confidence interval	Linear	95% confidence interval	Exponential	95% confidence interval
1	1.46	1.40–1.53	1.02	0.95–1.11	1.48	1.41–1.57	1.06	1.01–1.12	1.25	1.19–1.32	0.99	0.91–1.08
2	1.43	1.37–1.50	1.04	1.00–1.09	1.66	1.62–1.70	1.21	1.16–1.26	1.24	1.20–1.29	0.97	0.91–1.03
3	2.24	2.17–2.32	1.30	1.21–1.40	2.02	1.84–2.25	1.31	1.22–1.40	1.99	1.92–2.06	1.36	1.15–1.67
4	1.34	1.18–1.56	0.92	0.75–1.17	1.15	1.08–1.23	0.75	0.55–1.17	1.36	1.31–1.42	1.05	0.97–1.15
5	2.45	1.89–3.51	1.42	1.08–2.06	2.00	1.97–2.03	1.47	1.40–1.55	1.66	1.51–1.84	1.41	1.25–1.63
6	1.44	1.39–1.49	1.10	1.06–1.14	1.31	1.26–1.36	1.01	0.95–1.07	1.35	1.31–1.40	1.18	1.15–1.21
7	1.30	1.16–1.47	1.26	0.98–1.76	1.17	1.06–1.29	0.81	0.66–1.06	1.29	1.06–1.65	1.20	0.96–1.58
8	2.07	2.02–2.12	1.26	1.22–1.30	1.92	1.66–2.30	1.26	0.89–2.15	1.62	1.56–1.69	1.26	1.14–1.41
9	1.53	1.50–1.55	0.91	0.89–0.94	1.50	1.47–1.53	0.98	0.96–1.00	1.64	1.34–2.10	0.92	0.76–1.18
10	3.04	2.89–3.20	1.82	1.64–2.05	2.43	2.17–2.77	1.31	1.19–1.45	2.38	1.73–3.84	1.44	0.96–2.86
11	2.18	2.09–2.27	1.50	1.38–1.64	1.99	1.60–2.63	1.39	1.29–1.49				
12	1.67	1.59–1.77	1.02	0.94–1.12	1.62	1.60–1.64	1.01	0.97–1.06	1.89	1.72–2.11	1.33	1.15–1.58
13	1.13	1.09–1.18	0.98	0.92–1.04	1.21	1.16–1.26	1.02	0.97–1.08				
14	1.07	1.04–1.10	0.88	0.81–0.96	1.02	0.99–1.05	0.78	0.74–0.83	1.34	1.26–1.42	1.31	1.11–1.59
15	0.92	0.89–0.95	0.81	0.74–0.90	0.89	0.79–1.02	0.77	0.56–1.21				
Reference flux			1	0.94–1.07			1	0.90–1.17			1	0.88–1.16

using the same calibration system as in this study Pumpanen et al. (2004) reported that the standard error of CO<sub>2</sub> flux measurements from adjacent chambers was between 2 and 17% of the mean flux, and the vertical flux through the sand bed was considered spatially homogenous and not biased significantly by horizontal transport.

#### 4.4. Applicability of the results

Overall, the majority of chambers in the experiment lead to underestimations of the fluxes because of the chamber design, or the use of an improper flux calculation method. Our results indicate that the static chamber methodologies widely used in Europe inherently bias the accuracy in terms of measuring the exchange of trace gases between the soil and the atmosphere.

Generally, it is always difficult to extrapolate results from a laboratory experiment to the field conditions. Also, the applicability of the results depends on the measurement site, measurement setup and accuracy of the flux measurement. With respect to soil porosity, quartz sand simulates mineral soil rather well, and the results could be applied in grasslands, agricultural soils and some forest soils with no extended organic layer (Grünzweig et al., 2003). In forests, however, the soil surface is usually more porous as the porosity in the humus layer can exceed 80%. Thus, air currents move even more easily in forest soil than in quartz sand, and the disturbance of a chamber on the soil–atmosphere gas exchange may be very different. Our experiment showed that the chamber fluxes ( $F_{\text{lin}}$  and  $F_{\text{exp}}$ ) and the reference fluxes ( $F_{\text{ref}}$ ) tended to be smaller when measuring the fluxes with the smallest soil porosity (S3). Also, we found that the chamber specific flux underestimation was greater,  $R_{\text{exp}}$  but not  $R_{\text{lin}}$ , when measuring fluxes with the S3 as compared to the soils with higher soil porosities. This finding may be an artefact due to the fact that the biggest chamber(s) did not have measurements with S3, misbalancing the comparison of chamber fluxes to the reference fluxes. Hence, based on our results it is not possible to draw conclusions of the effects of soil types on chamber specific flux underestimation. However, as there is contradicting evidence that the flux underestimation by static chambers should increase with increasing soil porosity due to the storage of the target gas underneath the chamber (Conen and Smith, 2000), the possible influences of soil types, or porosities, on chamber specific under- or overestimations should be further investigated.

In several ecosystems the fluxes of CH<sub>4</sub> are often negative or lower than those measured in this study (e.g. Skiba et al., 2009). Hence, one should be careful when extrapolating our results outside the flux range (200–2300  $\mu\text{g CH}_4 \text{ m}^{-2} \text{ h}^{-1}$ ) of the study, although the experiment showed that the chamber-specific under- or overestimations were independent of the flux level.

As our experimental setup does not allow to estimate the effect of headspace mixing by fans, we assume that the conclusions drawn by Christiansen et al. (2011) that the use of a fan improves the flux estimation and decreases uncertainty in the flux, applies also for a larger group of chambers. This is especially true for chamber measurements conducted on bare soil as were the conditions in the experiment. Any method of headspace mixing creates turbulence within the chamber headspace. In order to mimic pre-deployment turbulent conditions, one should adjust the speed of mixing accordingly. This would, however, require near-surface wind speed measurements, and in changing conditions, or under for instance dense vegetation this would be rather challenging. We consider that the effect of headspace mixing and the speed of the headspace mixing would be timely topics for a new measurement campaign.

The correction factors for linear and exponential flux calculation methods show the over- or underestimations of the fluxes of individual chambers and groups of chambers based on chamber size. These correction factors can be used to correct for

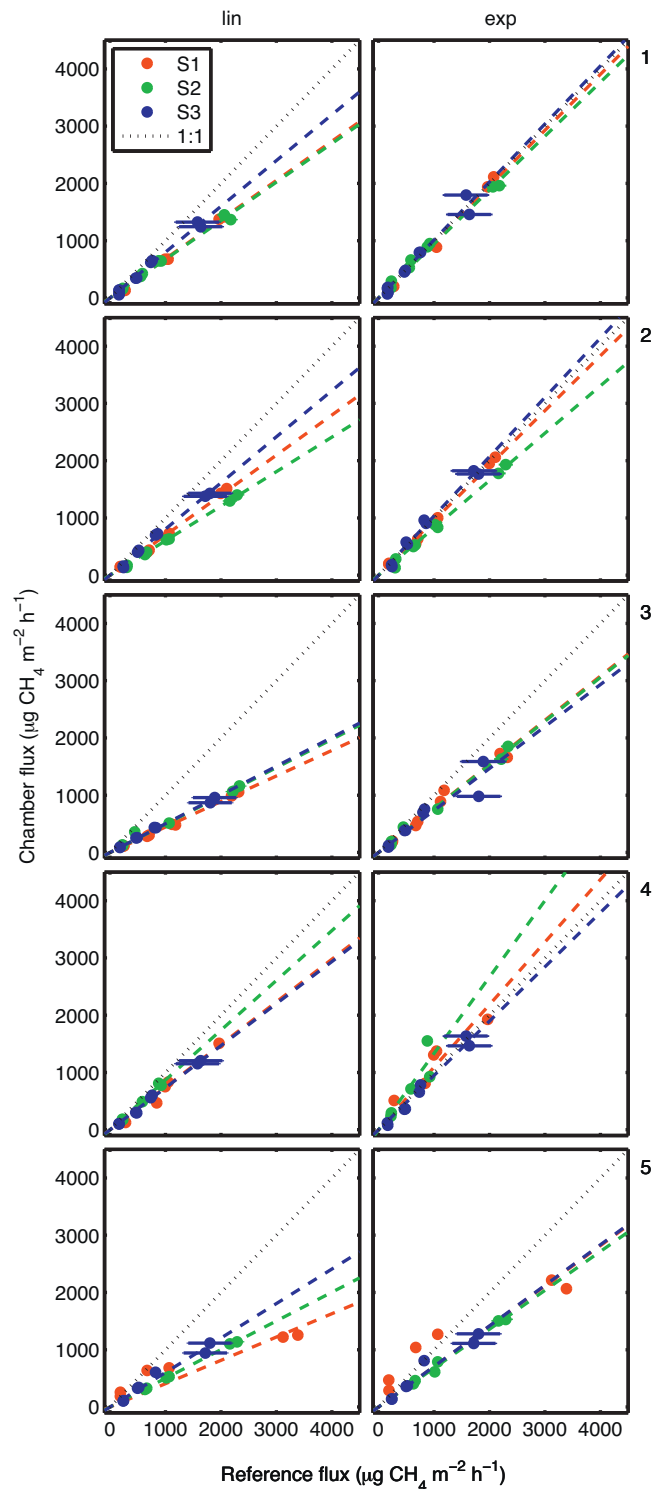


**Fig. A1.** Chamber fluxes vs. reference fluxes ( $\mu\text{g CH}_4 \text{ m}^{-2} \text{ h}^{-1}$ ) of CH<sub>4</sub> plotted for each chamber over all four flux levels. Different colors represent different sand types: fine dry sand (S1), coarse dry sand (S2) and fine wet sand (S3), and two parallel plots show results based on linear and exponential fits. With two or less measurement points, the regression was not fitted through the data, but the data points are visible. The chamber number is given on the right of each plot. Full colored lines represent linear regression lines forced through zero for each sand type. Error bar in the reference fluxes stand for 95% confidence intervals.

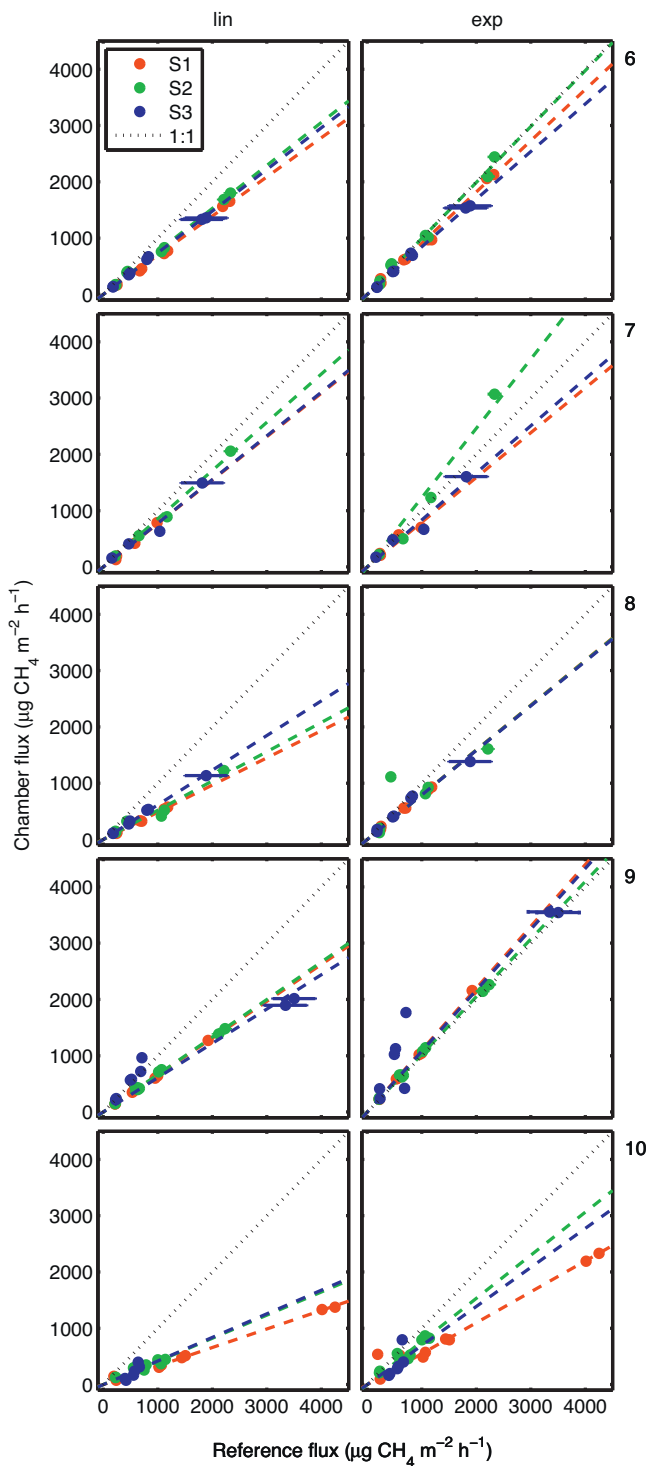


Fig. A1. (Continued)

the under- or overestimation of the fluxes by the individual chambers, however, they should be applied only under similar conditions as those in the study. An important notice is that the correction factors are based on the comparison of reference fluxes calculated by exponential calculation method against chamber fluxes calculated by (1) linear calculation method, and (2) exponential calculation method. The reference flux used for the comparison is taken from the time of the chamber closure, which better fits to the comparison of the exponential chamber flux (calculated for the time of chamber closure). Therefore,

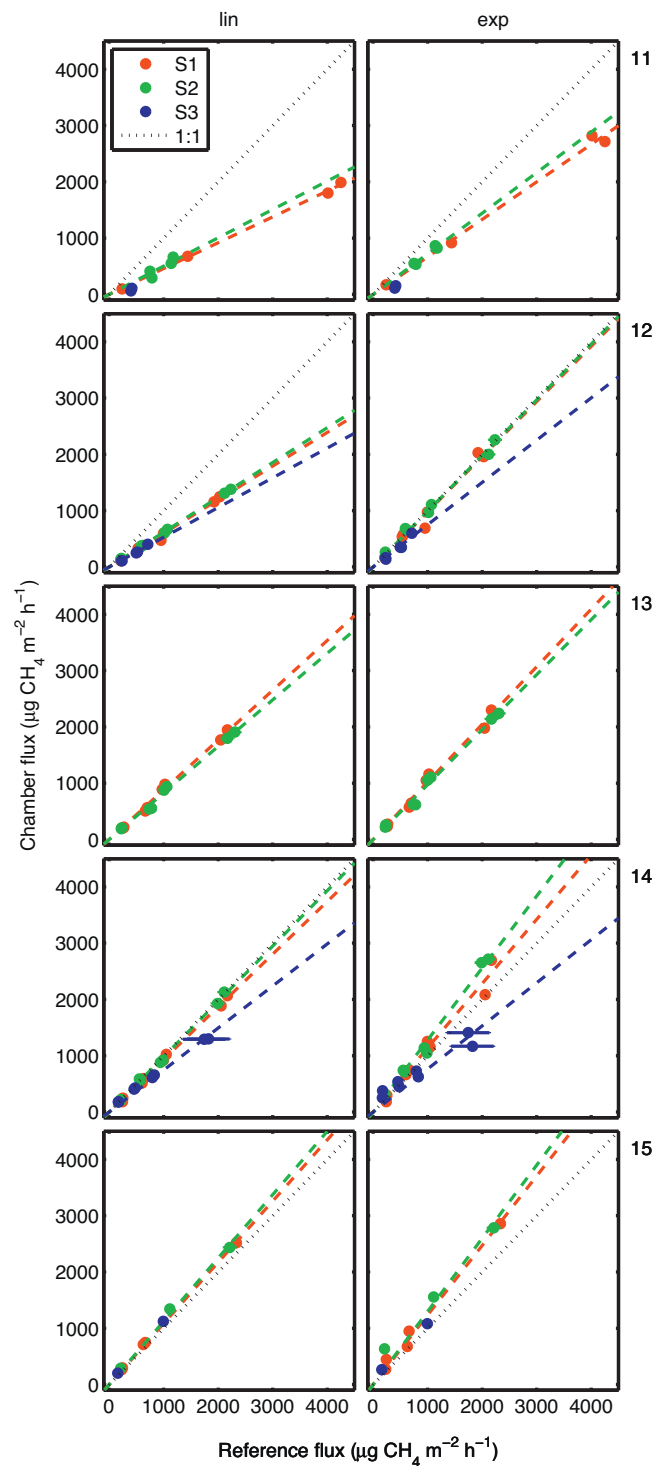


Fig. A1. (Continued)

the comparison of the reference flux to the linear chamber flux probably provides an upper limit to the possible underestimation of the fluxes, and therefore also the correction factors may be biased.

## 5. Conclusions

Our experiment shows that the linear flux calculation method consistently leads to underestimated  $\text{CH}_4$  fluxes from the soil, whereas the exponential flux calculation method gives more

accurate flux estimates, however, it increases the uncertainty. The underestimation of the fluxes was independent of flux level, but decreased with increasing chamber height ( $h$ ), area ( $A$ ) and volume ( $V$ ). As our objective was to assess uncertainties and errors of chamber measurements, and to explain them by chamber design and flux calculation methods, we conclude that chamber design (height, area, volume) explained some of the errors related to chamber measurements, and the use of a non-linear flux calculation method improved the flux estimation. However, still high uncertainties remain and not all the under- or overestimations of the tested chambers could be explained by the factors tested in our experiment.

## Acknowledgements

We wish to thank the staff at the Hyytiälä forestry field station for letting us occupy the storage hall for the campaign. Special thanks go to Heikki Laakso for setting up the data collection system for the calibration system, and for Sirkka Lietsala for conducting part of the GC analysis. This research was financially supported by Nitrogen in Europe (NinE) program of the European Science Foundation (ESF), COST Action 639 under ESF, ACCENT BIAFLUX EU-project, GREENFLUX-TOK project “*Micrometeorological techniques for In-situ measurements of greenhouse gases*” (contract no. MTKD-CT-2006-042445), Maj and Tor Nessling Foundation, and the Academy of Finland Centre of Excellence program (project number 1118615), the post-doctoral project 1127756, and the Academy Fellow project 130984. The EU FP6 NitroEurope IP also supported many of the participants during their visit to Hyytiälä.

## Appendix A.

see Fig. A1 and Table A1.

## References

- Anthony, W.H., Hutchinson, G.L., Livingston, G.P., 1995. Chamber measurement of soil-atmosphere gas exchange: linear vs. diffusion-based flux models. *Soil Sci. Soc. Am. J.* 59, 1308–1310.
- Butnor, J.R., Johnsen, K.H., 2004. Calibrating soil respiration measures with a dynamic flux apparatus using artificial soil media of varying porosity. *Eur. J. Soil Sci.* 55, 639–647.
- Christiansen, J.R., Korhonen, J.F.J., Juszczak, R., Giebels, M., Pihlatie, M., 2011. Assessing the effects of chamber placement, manual sampling and headspace mixing on  $\text{CH}_4$  fluxes in a laboratory experiment. *Plant Soil* 343, 171–185.
- Conen, F., Smith, K.A., 2000. An explanation of linear increases in gas concentration under closed chambers used to measure gas exchange between soil and the atmosphere. *Eur. J. Soil Sci.* 51, 111–117.
- Corley, J., 2003. Best practices in establishing detection and quantification limits for pesticide residues in foods. In: Lee, P.W., Aizawa, H., Barefoot, A.C., Murphy, J.J. (Eds.), *Handbook of Residue Analytical Methods for Agrochemicals*. John Wiley & Sons, New York, pp. 1–18.
- Davidson, E.A., Savage, K., Verchot, L.V., Navarro, R., 2002. Minimizing artifacts and biases in chamber-based measurements of soil respiration. *Agric. For. Meteorol.* 113, 21–37.
- Forbrich, I., Kutzbach, L., Hormann, A., Wilmking, M., 2010. A comparison of linear and exponential regression for estimating diffusive  $\text{CH}_4$  fluxes by closed-chambers in peatlands. *Soil Biol. Biochem.* 42, 507–515.
- Gao, F., Yates, S.R., 1998a. Simulation of enclosure-based methods for measuring gas emissions from soil to the atmosphere. *J. Geophys. Res.* 103 (D20), 26127–26136.
- Gao, F., Yates, S.R., 1998b. Laboratory study of closed and dynamic flux chambers: Experimental results and implications for field application. *J. Geophys. Res. Atmos.* 103, 26115–26125.
- Grünzweig, J.M., Totenberg, E., Yakir, D., 2003. Carbon sequestration in arid-land forest. *Global Change Biol.* 9, 791–799.
- Hutchinson, G.L., Mosier, A.R., 1981. Improved soil cover method for field measurement of nitrous oxide fluxes. *Soil Sci. Soc. Am. J.* 45, 311–316.
- Hutchinson, G.L., Livingston, G.P., 2001. Vents and seals in non-steady-state chambers used for measuring gas exchange between soil and the atmosphere. *Eur. J. Soil Sci.* 52, 675–682.
- Kroon, P.S., Hensen, A., Van den Bulk, W.C.M., Jongejan, P.A.C., Vermeulen, A.T., 2008. The importance of reducing the systematic error due to non-linearity in  $\text{N}_2\text{O}$  flux measurements by static chambers. *Nutr. Cycl. Agroecosyst.* 82, 175–186.
- Kutzbach, L., Schneider, J., Sachs, T., Giebels, M., Nykänen, H., Shurpali, N.J., Martikainen, P.J., Alm, J., Wilmking, M., 2007.  $\text{CO}_2$  flux determination by closed-chamber methods can be seriously biased by inappropriate application of linear regression. *Biogeosciences* 4, 1005–1025.
- Lai, D.Y.F., Roulet, N.T., Humphreys, E.R., Moore, T.R., Dalva, M., 2012. The effect of atmospheric turbulence and chamber deployment period on autochamber  $\text{CO}_2$  and  $\text{CH}_4$  flux measurements in an ombrotrophic peatland. *Biogeosciences* 9, 3305–3322.
- Levy, P.E., Gray, A., Leeson, S.R., Gaiawyn, J., Kelly, M.P.C., Cooper, M.D.A., Dinsmore, K.J., Jones, S.K., Sheppard, L.J., 2011. Quantification of uncertainty in trace gas fluxes measured by the static chamber method. *Eur. J. Soil Sci.* 62, 811–821.
- Livingston, G.P., Hutchinson, G.L., 1995. Enclosure-based measurement of trace gas exchange: application and sources of error. In: Matson, P.A., Harriss, R.C. (Eds.), *Biogenic Trace Gases: Measuring Emissions from Soil and Water*. Backwell Science, Cambridge, pp. 14–50.
- Livingston, G.P., Hutchinson, G.L., Spartalian, K., 2005. Diffusion theory improves chamber-based measurements of trace gas emissions. *Geophys. Res. Lett.* 32, L24817.
- Livingston, G.P., Hutchinson, G.L., Spartalian, K., 2006. Trace gas emission in chambers: a non-steady-state diffusion model. *Soil Sci. Soc. Am. J.* 70, 1459–1469.
- Matthias, A.D., Yarger, D.N., Weinbeck, R.S., 1978. A numerical evaluation of chamber method for determining gas fluxes. *Geophys. Res. Lett.* 5, 765–768.
- Nay, S.M., Mattson, K.G., Bormann, B.T., 1994. Biases of chamber methods for measuring soil  $\text{CO}_2$  efflux demonstrated with a laboratory apparatus. *Ecology* 75, 2460–2463.
- Pedersen, A.R., Petersen, S.O., Schelde, K., 2010. A comprehensive approach to soil-atmosphere trace-gas flux estimation with static chambers. *Eur. J. Soil Sci.* 61, 888–902.
- Pumpanen, J., Kolari, P., Ilvesniemi, H., Minkinen, K., Vesala, T., Niinisto, S., Lohila, A., Larmola, T., Morero, M., Pihlatie, M., Janssens, I., Yuste, J.C., Grunzweig, J.M., Reth, S., Subke, J.A., Savage, K., Kutsch, W., Ostreng, G., Ziegler, W., Anthoni, P., Lindroth, A., Hari, P., 2004. Comparison of different chamber techniques for measuring soil  $\text{CO}_2$  efflux. *Agric. For. Meteorol.* 123, 159–176.
- Pumpanen, J., Longdoz, B., Kutsch, W.L., 2009. Chapter 2. Field measurements of soil respiration: principles and constraints, potentials and limitations of different methods. In: Kutsch, W.L., Bahn, M., Heinemeyer, A. (Eds.), *Soil Carbon Dynamics – An Integrated Methodology*. pp. 16–33. Cambridge University Press. ISBN 978-0-521-86561-6 Hardback.
- Rochette, P., Eriksen-Hamel, N.S., 2008. Chamber measurements of soil nitrous oxide flux: Are absolute values reliable? *Soil Sci. Soc. Am. J.* 72, 331–342.
- Skiba, U., Drewer, J., Tang, Y.S., van Dijk, N., Helfter, C., Nemitz, E., Fumari, D., Cape, J.N., Jones, S.K., Twigg, M., Pihlatie, M., Vesala, T., Larsen, K.S., Carter, M.S., Ambus, P., Ibrom, A., Beier, C., Hensen, A., Frumau, A., Erisman, J.W., Brüggemann, N., Gasche, R., Butterbach-Bahl, K., Neftel, A., Spirig, C., Horvath, L., Freibauer, A., Cellier, P., Laville, P., Loubet, B., Magliulo, E., Bertolini, T., Seufert, G., Andersson, M., Manca, G., Laurila, T., Aurela, M., Lohila, A., Zechmeister-Boltenstern, S., Kitzler, B., Schauffler, G., Siemens, J., Kindler, R., Flechard, C., Sutton, M.A., 2009. Biosphere-atmosphere exchange of reactive nitrogen and greenhouse gases at the NitroEurope core flux measurement sites: Measurement strategy and first data sets. *Agric. Ecosyst. Environ.* 133, 139–149.
- Venterea, R.T., Baker, J.M., 2008. Effects of soil physical nonuniformity on chamber-based gas flux estimates. *Soil Sci. Soc. Am. J.* 72, 1410–1417.
- Venterea, R.T., Spokas, K.A., Baker, J.M., 2009. Accuracy and precision analysis of chamber-based nitrous oxide gas flux estimates. *Soil Sci. Soc. Am. J.* 73, 1087–1093, <http://dx.doi.org/10.2136/sssaj2008.0307>.
- Vicca, S., Fizev, L., Kockelbergh, F., Van Pelt, D., Segers, J.J.R., Meire, P., Ceulemans, R., Janssen, I.A., 2009. No signs of thermal acclimation of heterotrophic respiration from peat soils exposed to different water levels. *Soil Biol. Biochem.* 41, 2014–2016.
- Widen, B., Lindroth, A., 2003. A calibration system for soil carbon dioxide efflux measurement chambers: description and application. *Soil Sci. Soc. Am. J.* 67, 327–334.
- Xu, L., Furtaw, M.D., Madsen, R.A., Garcia, R.L., Anderson, D.J., McDermitt, D.K., 2006. On maintaining pressure equilibrium between a soil  $\text{CO}_2$  flux chamber and the ambient air. *J. Geophys. Res.* 111, D08S10, <http://dx.doi.org/10.1029/2005JD006435>.